Brain Structure and Function (2020) 225:71–84
https://doi.org/10.1007/s00429-019-01984-9

ORIGINAL ARTICLE

Mapping the community structure of the rat cerebral cortex with weighted stochastic block modeling

Joshua Faskowitz[1,2] · **Olaf Sporns**[1,2,3]

Received: 24 April 2019 / Accepted: 9 November 2019 / Published online: 23 November 2019

Abstract

The anatomical architecture of the mammalian brain can be modeled as the connectivity between functionally distinct areas of cortex and sub-cortex, which we refer to as the *connectome*. The community structure of the connectome describes how the network can be parsed into meaningful groups of nodes. This process, called community detection, is commonly carried out to find internally densely connected communities—a modular topology. However, other community structure patterns are possible. Here we employ the weighted stochastic block model (WSBM), which can identify a wide range of topologies, to the rat cerebral cortex connectome, to probe the network for evidence of modular, core, periphery, and disassortative organization. Despite its algorithmic flexibility, the WSBM identifies substantial modular and assortative topology throughout the rat cerebral cortex connectome, significantly aligning to the modular approach in some parts of the network. Significant deviations from modular partitions include the identification of communities that are highly enriched in core (rich club) areas. A comparison of the WSBM and modular models demonstrates that the former, when applied as a generative model, more closely captures several nodal network attributes. An analysis of variation across an ensemble of partitions reveals that certain parts of the network participate in multiple topological regimes. Overall, our findings demonstrate the potential benefits of adopting the WSBM, which can be applied to a single weighted and directed matrix such as the rat cerebral cortex connectome, to identify community structure with a broad definition that transcends the common modular approach.

Keywords Connectome · Community structure · Stochastic block model · Rat cortex · Modularity

Introduction

The mammalian brain is characterized by complex patterns of connectivity (Sporns 2011; Park and Friston 2013). This connectivity can be comprehensively described by creating a network model of the brain's wiring—an account of the patterns of connectivity between distinct regions, referred to as the *connectome* (Sporns et al. 2005). Using the tools of network science, we can quantitatively analyze and model the connectome to characterize statistical properties of its organization (Bassett and Sporns 2017). A long series of prior studies of anatomical brain networks across several different species have revealed a consistent set of attributes, such as heavy-tailed degree distributions, a prevalence of specific classes of subgraphs or motifs, as well as the existence of densely connected network communities or modules (Sporns and Betzel 2016).

It is increasingly recognized that brain networks exhibit significant features of organization on multiple scales (Betzel and Bassett 2017). Of particular interest is the so-called mesoscale of organization, a level of analysis that describes network properties falling between node statistics (e.g., degree, clustering coefficient, or centrality) and global statistics (e.g., network density or efficiency) (Sporns 2013; Tunç and Verma 2015). A particularly important mesoscale organizational property of a connectome is the way in which its nodes can be grouped into distinct communities. Modular organization is

Electronic supplementary material The online version of this article (https://doi.org/10.1007/s00429-019-01984-9) contains supplementary material, which is available to authorized users.

✉ Joshua Faskowitz
jfaskowi@iu.edu

[1] Program in Neuroscience, Indiana University, Bloomington, IN, USA

[2] Department of Psychological and Brain Sciences, Indiana University, 1101 E. 10th Street, Bloomington, IN 47405, USA

[3] Indiana University Network Science Institute, Indiana University, Bloomington, IN, USA

of neurobiological interest as members of communities often share other common attributes, such as geometric placement and contiguity, functional specialization, and developmental and evolutionary origin (Sporns and Betzel 2016). In other words, the community structure of a network is an organizational scale that can be used to identify meaningful groups of nodes based on patterns of connectivity or coactivation. Such node groups could function to support a specific cognitive domain (Crossley et al. 2013). Information about this community structure may also be used to classify brains into clinical groups (Kurmukov et al. 2017; He et al. 2018). Brain network communities have been found in species as diverse as the nematode *C. elegans* (Sohn et al. 2011), the fruit fly *Drosophila melanogaster* (Shih et al. 2015), mouse (Zingg et al. 2014; Rubinov et al. 2015), rat (Bota et al. 2015; Swanson et al. 2016; Swanson et al. 2017; Swanson et al. 2018), and rhesus monkey (Harriger et al. 2012).

Network communities can be detected by global maximization of a modularity metric (Newman 2006), which by design identifies collections of nodes densely connected within each community and sparsely connected between communities. This approach of *modularity maximization* has been widely applied to brain network data, across many species and anatomical subdivisions of the brain. For example, anatomical modules in the human brain have been mapped across development (Baum et al. 2017) and the lifespan (Zhao et al. 2015), as well as in numerous clinical conditions such as degenerative (Contreras et al. 2019) and mental disorders (Alexander-Bloch et al. 2012). Modular organization of brain networks has been theorized to conserve anatomical wiring cost (Bullmore and Sporns 2012; Betzel et al. 2017) and to promote efficient embedding in physical space (Bassett et al. 2010).

Despite its popularity, modularity maximization is subject to several important limitations. Recent work emphasizes that a single modular partition may represent only one solution to a problem with no universally optimal approach (Fortunato and Hric 2016; Peel et al. 2017). Most complex networks have numerous plausible modular partitions that nearly maximize the modularity heuristic (Fortunato and Barthelemy 2007; Good et al. 2010) and, thus, it is not guaranteed that any single modular partition of the data is truly representative of the data. Furthermore, one partition or scale might not adequately capture the richness of the network organization (Betzel and Bassett 2017). Recent methodological advances have allowed accessing modular organization at multiple scales, through implementing modularity maximization while varying a resolution parameter that renders the modularity metric sensitive to modules of different sizes (Jeub et al. 2018).

To ascribe importance to any one partition without considering other 'just as plausible' partitions could lead to misinterpretations of a connectome's community structure. Two different analytical approaches address such concerns: (1) a representative community structure from a landscape of community structures, either using a representative partition (Meunier et al. 2009) or a consensus method (Lancichinetti and Fortunato 2012), can be chosen; or (2) analysis can be performed on a set of many plausible community structure realizations of an algorithm (Betzel et al. 2019).

Furthermore, communities need not necessarily or exclusively satisfy the condition of dense intra-community and sparse inter-community connectivity; groups of nodes can also be grouped into communities based on graph-cuts, states or types of dynamics, or statistical models (Schaub et al. 2017). Here, we are specifically interested in brain network communities identified within the framework of stochastic block models (SBM) (Holland et al. 1983; Aicher et al. 2014; Moyer et al. 2015a, b; Faskowitz et al. 2018). The SBM is an edge-generative model that describes how communities connect to each other on average. An SBM community of nodes, referred to as a *block*, can be thought of as a group of nodes who connect to other communities in a similar (i.e., stochastically equivalent) manner. By this design, the SBM is flexible; it can describe a range of community structure topologies, such as core-periphery (Pavlovic et al. 2014; Noori et al. 2017; Battiston et al. 2018) or disassortative (Betzel et al. 2018), in addition to modular communities.

Spurred by recent advances in neuroinformatics, the anatomical wiring of the rat at the scale of areas and inter-areal connectivity has been assembled (Bota and Swanson 2007). Among the first anatomical subdivisions examined in the rat brain was the cerebral cortex (Bota et al. 2015), which appears to share fundamental network properties with primate cerebral cortex, such as the presence of a small-world, modular, and rich club organization (Bota et al. 2015; van den Heuvel et al. 2016). The community structure of the rat cerebral cortex reveals modules that are spatially compact and have meaningful relationships with functionally and behaviorally specialized systems. An SBM approach could potentially complement the insights gained from standard modularity maximization by revealing partitions based on a different set of criteria for defining module membership.

Here, we identify community structure in the rat cerebral cortex connectome with a weighted variant of the stochastic blockmodel (WSBM) (Aicher et al. 2013, 2014; Peixoto 2018). The goal of the present work is to demonstrate how the blockmodeling approach can be applied to a singular brain network in a manner that reveals a range of plausible topologies. In conjunction, we compare the blockmodeling approach to a more standard approach, modularity maximization, in these analyses. We find that WSBM can recover a consensus community structure with non-modular elements and we compare the resulting partitions to a classic modular community structure. We also show that this WSBM community structure is well suited to generate synthetic data.

We then use the range of plausible community structure partitions to assess the frequency at which nodes and edges participate in certain community structure topologies. Overall, our approach provides a novel framework for inferring and utilizing the WSBM to analyze a range of community structure topologies in anatomical brain network data. We identify evidence that the community structure of the rat cerebral cortex connectome contains non-modular organizational elements, including brain regions that participate in core, periphery, or even disassortative relationships.

Methods

The rat cerebral cortex connectome

The data set used for our analysis is derived from Swanson et al. (2017), referred to as version *RCAMv2*. Directed and weighted connectivity was assembled between 77 distinct cortical gray matter regions of the rat cortex, delineated based on architecture, topography, and connectivity (Swanson et al. 2016). Between these 77 regions, there are 5852 (77^2–77) potential edges to consider. Connection reports of monosynaptic anterograde and retrograde connections were recorded as an adjacency matrix. 2155 nonzero edges were recorded, with weights assigned on an ordinal scale, from 0 to 7 in the following way: absent, very weak, weak, weak–moderate, moderate, moderate–strong, strong, and very strong. As in prior work (Bota et al. 2015), this ordinal scale was transformed to a tapered log-weighted scale: {0, 0.0001, 0.001, 0.01, 0.075, 0.3, 0.75, 1.0}.

Stochastic blockmodel concepts

The stochastic blockmodel (SBM) is an edge-generative model for describing how groups of nodes interact with each other in a network. Importantly, a community as defined by an SBM is a group of nodes that connect to the rest of the network in a similar pattern. Specifically, nodes in the same community will, on average, have the same connectional profile to other communities (for an alternative analysis of node-level connectional similar, see Supplemental Information). This property is referred to as stochastic equivalence. The SBM can generate a network by assigning a probability of connection for all possible pairs of communities (including within-community [modular] interactions). In the classic SBM, this probability, Θ, is governed by a Bernoulli distribution. The collection of Θ that describes the probability of connection between each community is the affinity matrix, B. For an SBM describing k communities, B will be of size $k \times k$.

This stochastic block modeling framework serves as a general model that can be extended for specialized purposes, such as blockmodels with mixed membership (Airoldi et al. 2008; Moyer et al. 2015a, b), degree correction (Karrer and Newman 2011; Xiaoran et al. 2014), and weighted edges (Peixoto 2018). For the present study, we utilize the weighted variant of the SBM, known as the WSBM (Aicher et al. 2013, 2014). The MATLAB (The MathWorks, Inc., Natick, Massachusetts) code implementing this WSBM is available at *tuvalu.santafe.edu/~aaronc/wsbm/*. We provide wrapper scripts useful for the application of the WSBM to brain networks at *github.com/faskowit/blockmodeltools*.

We use a Bernoulli distribution to describe edge existence between blocks and an exponential distribution to describe the weight distribution between blocks. The generative process of the WSBM can be summarized as follows:

- For each node, assign a community membership.
- For each pair of communities, assign edge existence and edge weight parameters.
- For each edge, draw from a Bernoulli distribution with the corresponding edge-existence parameter.
- For each existing edge, draw from an exponential distribution with the corresponding edge weight parameters.

We use a variational Bayes algorithm (Aicher et al. 2014) to infer a block structure on the empirical network. This algorithm uses a maximum a posteriori approach to identify the WSBM model, which includes the community structure and the parameters for each community interaction (edge and weight) that is likely to have generated the observed data. The model likelihood (expressed as the log likelihood for mathematical convenience) is expressed as $P = (E|M, z)$, where E is the empirical data, M is a parameterized block model and z is the community assignment vector. The number of communities k is a free parameter of the WSBM model. Therefore, picking a k value for the WSBM amounts to a model selection problem. In this project, we fit models from a range of $k = \{2, 3, \ldots 20\}$.

As with many community detection methods, the WSBM is stochastic, yielding many community structure configurations after multiple algorithmic trials. As such, we explore two analytical paths: (1) resolve a consensus model from various community structure realizations; or (2) analyze patterns across various community structure realizations. In what follows, we describe frameworks for both approaches (Fig. 1).

Constructing consensus community structures

We designed a workflow to infer the WSBM in a consensus manner (Lancichinetti and Fortunato 2012; Faskowitz et al. 2018), to obtain a median solution from a landscape of plausible partitions. First, we select the optimal k-level to investigate based on the model likelihoods (Aicher et al. 2014). At

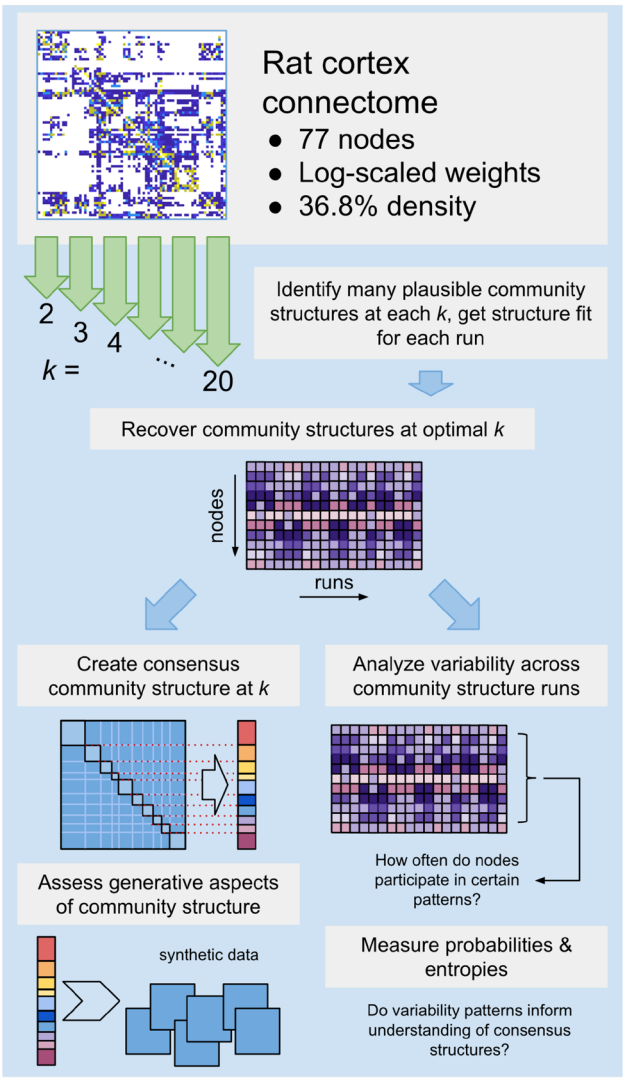

Fig. 1 Diagrammatic overview of the methods and analyses employed in this study

this k level, we identify an ensemble of N partitions and we measure the pairwise variation of information (VI) (Meilă 2007) between them. We identify the N_q partitions that had less than median VI distance and greater than median model log evidence to obtain well fit and reasonably central partitions from the landscape of N solutions. Of N_q partitions, we identify the centroid (least distant) partition and align the other $N_q - 1$ partitions to it using Jaccard distance (Munkres 1957). We then create a prior for each node's community affiliation based on the frequency of community assignment for each node across the N_q aligned partitions. We then infer the WSBM community structure 100 more times, using the generated prior to initialize the inference. This process is iterated until the agreement across 100 inferred partitions reaches a predefined level (Kwak et al. 2009). We retain the resultant model as the consensus WSBM community structure.

Modular model for comparison

We sought to compare the consensus WSBM community structure to a modular community structure at each scale k. We identify plausible modular community structures at multiple scales by sweeping across values of the γ parameter in the modularity equation. From a range of γ (from 0.01 to 4.0 in steps of 0.01, resulting in 400 γ values), we obtain communities using the Louvain method implemented in the Brain Connectivity Toolbox (Blondel et al. 2008; Rubinov and Sporns 2010). Then, for each level of k, we record the lowest and highest γ value that generates a partition with k communities. Within this range, we then uniformly randomly sample an ensemble of γ values used to obtain N partitions, therefore matching the ensemble size obtained from WSBM runs at each level of k.

Generative modeling methods

We use a previously established framework to measure how a generative model could create synthetic networks that vary minimally across several distributions of network properties (Betzel et al. 2016). A WSBM models how each community connects to all other communities. We can sample from these distributions to create synthetic data adhering to the model parameters. For each synthetic network, we record five network statistic distributions: directed weighted degree (strength), directed binary degree, weighted directed clustering coefficient, weighted node betweenness centrality, and binary node betweenness centrality. We include binary network metrics in this evaluation because edge existence (i.e., existence of edges between blocks, regardless of weight), is a network feature that the WSBM explicitly models. We then use Kolmogorov–Smirnov (KS) to measure the histogram distance between the synthetic distributions and the empirical distributions for the five network statistics. The difference between the synthetic and empirical networks can be indexed by the average of these five KS statistics; a lower mean KS signifies a more accurate match between synthetic and empirical networks. For this evaluation, we also create null generative models to evaluate against. The null models are created by randomly permuting the parameters of the intact model's affinity matrix. This procedure, therefore, retains the parameters of the original model, but the specific configuration of block interactions is permuted.

Community motif analysis

We also measure the diversity of community motifs across the many inferred WSBM models at each k (Betzel et al. 2018). This analysis entails measuring patterns of between-community (block interaction) connectivity w_{rs}, where w is the matrix of average edge strength between blocks, and

Table 1 Definitions for identifying community motif configurations for block matrix w

Community motif	Description	Definition
On-diagonal	Block represents within-community connectivity	w_{rs} when $r = s$
Assortative	Minimum on-diagonal value is larger than the off-diagonal value	$\min\left(w_{rr}, w_{ss}\right) > w_{rs}$
Core/periphery	Off-diagonal value is larger than one on-diagonal value; if the off-diagonal value is closer to the larger of the on-diagonal values, it is core; otherwise it is periphery	$\left(w_{rr} > w_{rs} > w_{ss}\right)$ or $\left(w_{ss} > w_{rs} > w_{rr}\right)$
Disassortative	Off-diagonal value is larger than both on-diagonal values	$w_{rs} > \max\left(w_{rr}, w_{ss}\right)$

where r and s are communities contained within the total set of k total communities, $\{r, s\} \in \{1, \ldots, k\}$. Community motifs are defined in Table 1.

For each community structure, we label each block interaction according to the definitions in Table 1. We then record which non-zero edges participate in each type of interaction, for each recovered partition. Measuring across partitions provides the frequency that an edge (a non-zero entry in the adjacency matrix) participates in each community motif. We conceptualize this frequency as a probability. From this edge-wise probability, we calculate an entropy metric (referred to in (Betzel et al. 2018) as a *diversity index*) that measures the probability for an edge (e) to participate in one or more of the community motifs:

$$\begin{aligned}\text{entropy}_e = -\big(&P_a \log_2 P_a + P_c \log_2 P_c + P_p \log_2 P_p \\ &+ P_d \log_2 P_d + P_{\text{od}} \log_2 P_{\text{od}}\big),\end{aligned}$$

where P_a, P_c, P_p, P_d and P_{od} stand for the probability of participating in an assortative, core, periphery, disassortative or on-diagonal relationship, respectively. To compute node entropy, we sum each node's edge entropy (in- and out- connections) and divide by two.

Results

Consensus community structure results

We fit the WSBM to the rat cortex connectome across a range of k and monitor when we reach a point of diminishing gains in model likelihood (Fig. 2a). We recovered 750 models (the target N) for $k = \{2, 3 \ldots 12\}$. Due to algorithm runtime, we recovered 500 models at $k = 13$, and 200 models at $k = \{14, 15\}$. At $k = \{16, 17 \ldots 20\}$, the WSBM inference tools struggle to recover models with the specified k. At these levels, only 91, 32, 53, 7, and 2 valid models were recovered. We sampled with replacement 100 models from the available recovered models at $k = \{16, 17 \ldots 20\}$.

To estimate the optimal k, we identified the scale at which model log evidence begins to decline as k grows. At each scale, we bootstrapped (10^4 iterations) the difference between mean model log evidence at k and $k + 1$. The transition at which the 99% confidence interval of these differences overlapped with 0 was taken to be a stopping criterion. This approach identified an optimum $k = 10$. At the $k = 10$ scale, we found that model log evidence relates to the mean VI distance (cross-validated $R^2 = 0.05$; Fig. 2b).

We obtained consensus community structures using two different approaches to community detection, each designed to parse a network based on different criteria: the WSBM and modularity maximization (Fig. 3). Supplemental Table 1 provides complete listings of rat cerebral cortex brain areas, arranged by community, for approach. Differences in the resulting consensus partitions are apparent when visualizing the average between-block density (i.e., average edge weight). The WSBM, as a statistical description of network communities, identifies communities with strong (e.g., community 6) as well as weak (e.g., communities 3, 7) on-diagonal density. The modular model, which optimizes the modularity metric, only identifies partitions with on-diagonal communities whose densities are, in all cases, stronger than any other off-diagonal interaction. Despite significant differences in the way communities are defined under the two approaches, the WSBM and modular consensus community structures are significantly less distant from each other than expected by chance (VI: 0.359; randomization test, 10^4 iterations, $p < 10^{-4}$). We compared how each of these structures concentrate edge weight in a modular manner, by evaluating the ratio of within on-diagonal blocks divided by edge weight between blocks: $M_{\text{ratio}} = \frac{\sum_{r=s} w_{rs}}{\sum_{r \neq s} w_{rs}}$. The modular structure has a $M_{\text{ratio}} = 0.846$ and the WSBM structure has a $M_{\text{ratio}} = 0.448$. The difference between these ratios was tested after randomizing the original rat cortex connectome data (with BCT function *randmio_dir_connected*) at edge rewiring probabilities of $p = \{0.25, 0.20, 0.15, 0.10, 0.05, 0.01\}$. For rewiring probabilities $0.25 - 0.05$, the empirical difference in M_{ratio} was at least greater than 95% of synthetically generated M_{ratio} values (10^4 iterations). We compared the modularity Q of the WSBM partition to synthetically generated Q values (rewiring the network with 0.05 probability, keeping partition order intact) and found that no synthetic values were greater than the empirical Q value (10^4 iterations).

We compared these consensus community structures to a previously published modular arrangement of these 77 nodes into three communities (Swanson et al. 2017) (Table 2). We

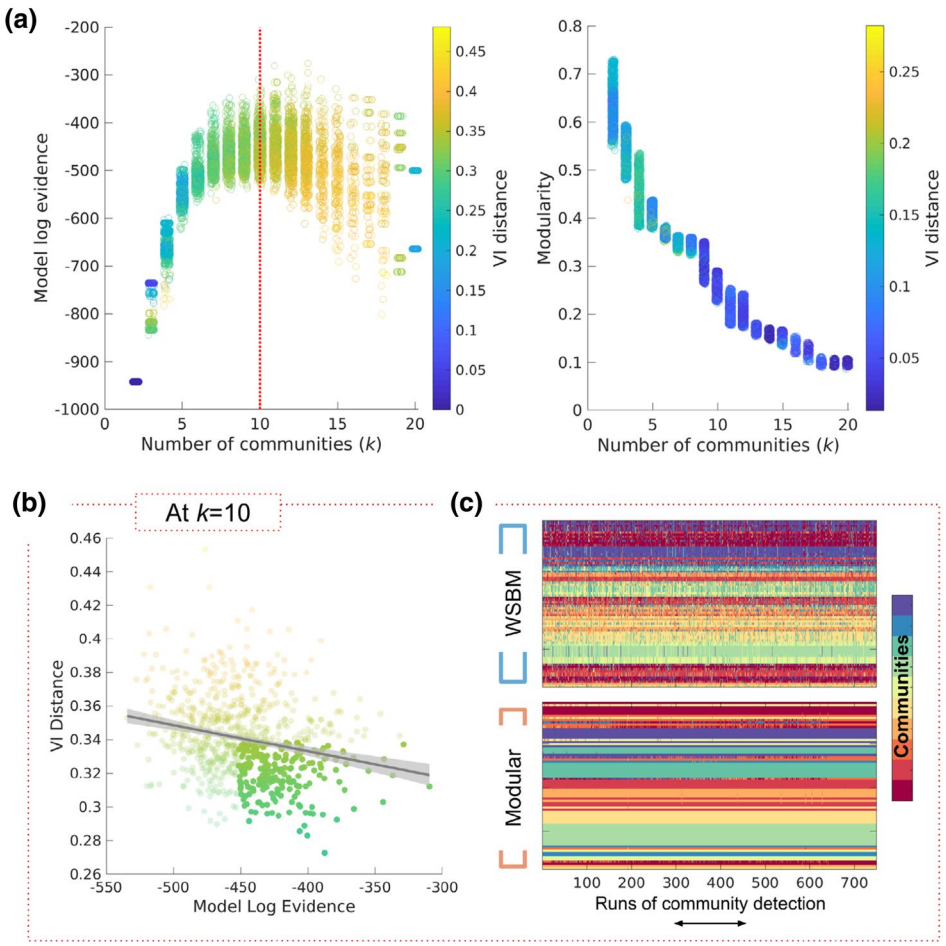

Fig. 2 Community detection results across the number of communities, k, parameter; **a** Scatter plots for WSBM (left) and modular (right) depicting the community recovered at each level of k; WSBM communities are plotted against model log evidence, modular communities are plotted against the Louvain algorithm's modularity metric; data points are colored by the average VI from one partition to all other partitions at k; the identified optimal $k = 10$ is denoted by a red vertical line in the WSBM plot; **b** The relationship between model log evidence and average VI distance, which explains 4.7% of the variance in model log evidence; points are colored by same scale as in **a**; opaque points indicate the models included in the construction of the consensus WSBM model; **c** 750 communities recovered using each method, aligned using the Munkres algorithm to a common structure for visualization

find that for the WSBM model, five out of ten communities are fully contained within one of the *Swanson2017* modules, while for the modular model, eight out of ten communities are fully contained within one of the *Swanson2017* modules. Divergence between the *Swanson2017* and WSBM partitions is greatest for WSBM communities 3, 4, and 9, which are communities with no more than two-thirds of the nodes co-classified to any one of the *Swanson2017* modules. These WSBM communities also maintain strong off-diagonal block interactions relative to their respective on-diagonal block interaction (Fig. 3). Six out of seven previously (Swanson et al. 2017) identified hub nodes (ENTl, AIp, PERI, ECT, BLAp, LA) are found in WSBM communities 2 and 4. All seven members of WSBM community 4 were previously identified as rich club areas (ENTl, ORBv, ORBm, MOs, PERI, ECT, CLA), with five more rich club areas found in community 2 (comprising half of its membership; CA1v, ILA, AIp, BLAp, LA), and the remaining three areas part of communities 3, 5 and 8. This high concentration of hubs/rich club areas in two WSBM communities indicates that the WSBM partition significantly captures the network's hub and rich club (or core-periphery) architecture.

Generative modeling results

When we fit a WSBM to network data, we obtain a generative model of the network based on the inferred community structure. We recorded the energy, computed as mean KS, between synthetic networks generated by the consensus WSBM and modular models. We find that the WSBM created synthetic data that deviated less from the empirical data than the modular generative model (Fig. 4a; bootstrapped difference of means, 10^4 iterations, $p < 10^{-4}$). Additionally, the difference between the WSBM energy distribution and its corresponding null distribution is greater than the difference between the modular counterparts (Fig. 4b; bootstrapped difference of differences, 10^4 iterations, $p < 10^{-4}$). Observing the individual measures that comprise the overall energy, we see that the WSBM model produces less divergent strength, binary degree, and betweenness centrality distributions, while the modular model produces less divergent clustering coefficient and binary betweenness centrality distributions (Fig. 4c).

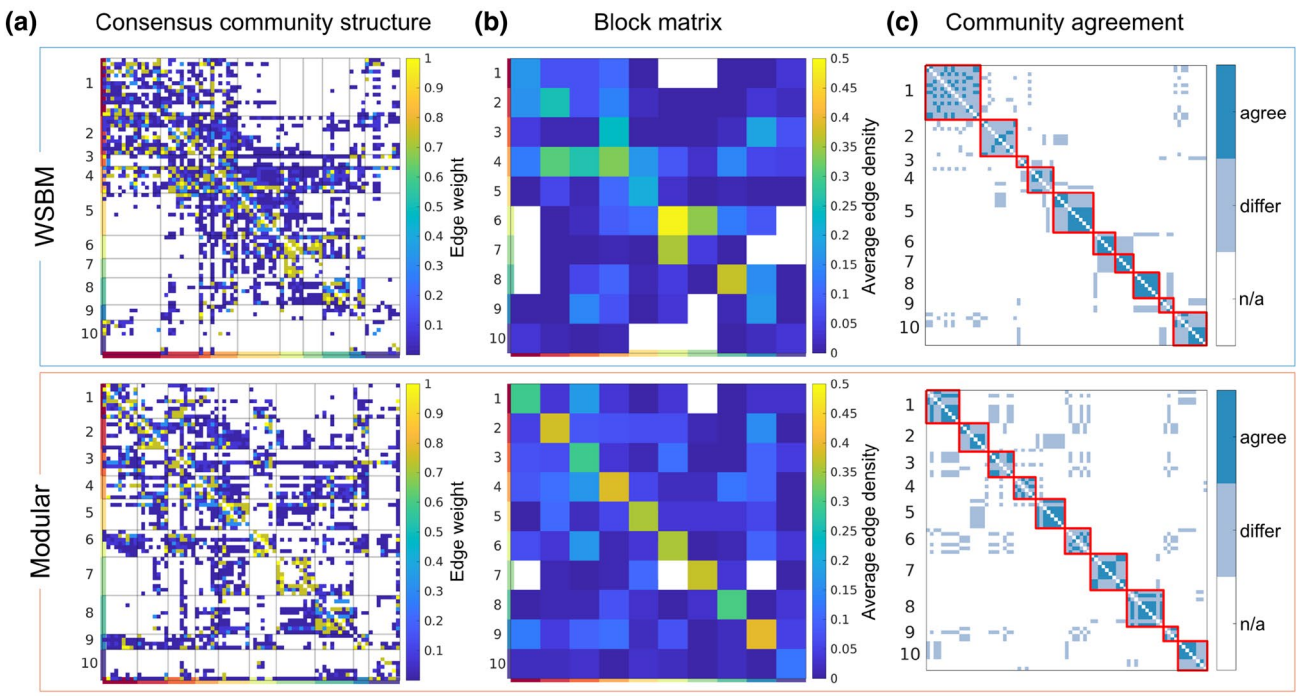

Fig. 3 Consensus community structures; **a** WSBM and modular consensus community structures at $k=10$; **b** Average block matrix for each community structure, depicting the average edge for each block interaction; areas in white indicate no edges present; **c** Agreement matrix between community structures, permuted by the order of each structure; *agree* classified in same community across structures, *differ* not in same community, *n/a* not applicable

Table 2 Node affiliations of WSBM and modular consensus community structures compared to a previously published community structure: *Swanson2017*

	WSBM communities									
	1	2	3	4	5	6	7	8	9	10
Swanson2017 Module 1	15	10	1	3	1	0	0	0	2	9
Swanson2017 Module 2	0	0	0	1	10	5	5	0	0	0
Swanson2017 Module 3	0	0	2	3	0	1	0	7	2	0
	Modular communities									
	1	2	3	4	5	6	7	8	9	10
Swanson2017 Module 1	9	5	7	1	0	7	0	0	4	8
Swanson2017 Module 2	0	3	0	0	8	0	10	0	0	0
Swanson2017 Module 3	0	0	0	5	0	0	0	10	0	0

Community motif results

Unlike classic modularity, WSBM builds on a considerably broader definition of network community that goes beyond assortative partitions. We can assess the extent to which certain community topology configurations occur by evaluating community motifs (Fig. 5a). Across 750 WSBM community structures at $k = 10$, we find instances of each type of community motif, whereas across 750 modular community structures, we observe only on-diagonal and assortative configurations (Fig. 5b). Concerning the motif probabilities derived from the WSBM model, 99.4% of edges participated in at least two community motifs across WSBM community structures. The top ten highest probability edges for the core, periphery, and disassortative community motifs are shown in Table 3.

In contrast, considering the motif probabilities derived from the modular model, 79.1% percent of nonzero edges displayed no variation in community motif configuration (100% on-diagonal: 247 edges; 100% assortative: 1458

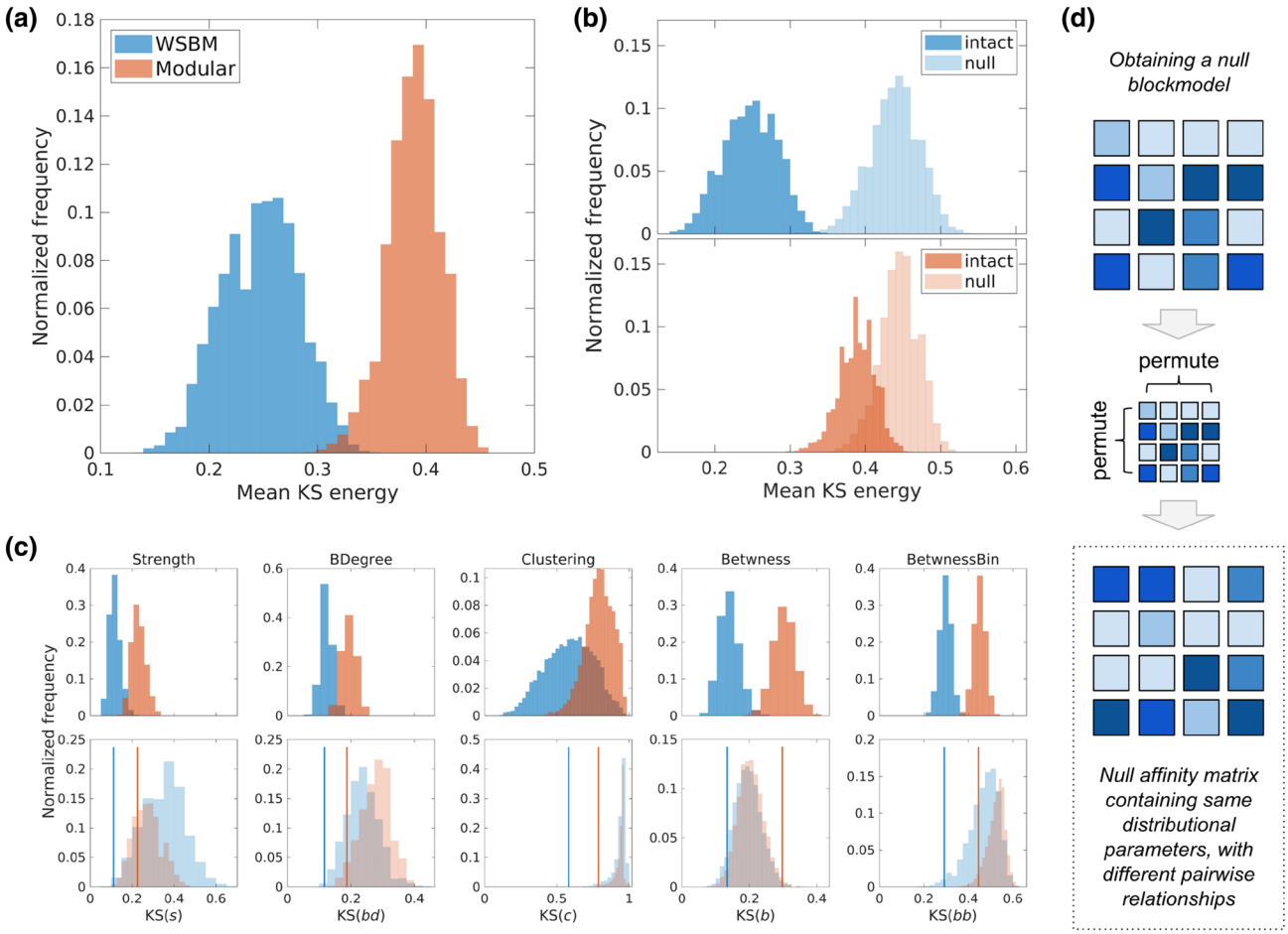

Fig. 4 Evaluation framework for synthetically generated networks by measuring Kolmogorov–Smirnov (KS) energy from empirical network; **a** Distribution of mean KS values of 10^4 generated networks from WSBM and modular community structures; **b** KS energy values of intact generative model versus permuted model (null); **c** Top: Individual KS distances for each network metric of the mean KS energy calculation; Bottom: Individual KS distances for each network metric of permuted model, with the median of the intact model distribution indicated with vertical line; **d** Schematic of how the generative model affinity matrix is permuted to create a 'null' generative model; note that the values of the inferred parameters are the same, but in new positions, introducing null community interactions

edges). 2 out of 10 modular communities were fully composed of on-diagonal nonzero edges with 100% on-diagonal participation (communities 7 and 10). 6 out of 10 modular communities were composed of nonzero edges with an average on-diagonal probability > 98% (communities 2, 4, 5, 6, 8, and 9).

For each edge, we recorded the highest probability motif (Fig. 5c, left). For each block interaction, we recorded the mode motif (Fig. 5c, right). The block matrix of motif modes classifies three block interactions as core ($4 \rightarrow 3$, $6 \rightarrow 7, 7 \rightarrow 6$), five block interactions as periphery ($2 \rightarrow 10$, $3 \leftrightarrow 3$, $3 \rightarrow 4$, $3 \rightarrow 10$, $4 \rightarrow 10$), and no block interactions as disassortative.

We observe higher overall community motif entropy for the WSBM model than for the modular model (Fig. 6, panel a). For the WSBM model, the greatest average between-block entropies involve community 4 ($4 \rightarrow 2$, $4 \rightarrow 3$). For the modular model, the greatest average between-block entropies concerned communities 1 and 3 ($3 \leftrightarrow 3$, $1 \leftrightarrow 1$, $1 \rightarrow 3$, and $3 \rightarrow 1$). Using a randomized block null model (like in Fig. 4d), we show that at random, node entropy is highly correlated with node degree (Fig. 6b; $\rho > 0.97$ for WSBM and modular). Community motif entropy measured across WSBM and modular partitions correlated with node degree substantially less than the entropy measured across random structure (WSBM $\rho = 0.85$, $p < 10^{-8}$; modular $\rho = 0.11$, not significant; for both models: difference between null and intact $p < 10^{-4}$). Further, we measured this change as a percentage change in entropy for each node (Supplemental Fig. 2). These patterns in entropy change are not correlated with node degree (WSBM ρ 95% confidence interval: $[-0.14,\ 0.27]$; modular ρ 95% confidence interval: $[-0.02,\ 0.42]$). At an edge wise scale, we observe that both WSBM ($\rho = 0.31$) and modular ($\rho = 0.21$) edge entropies

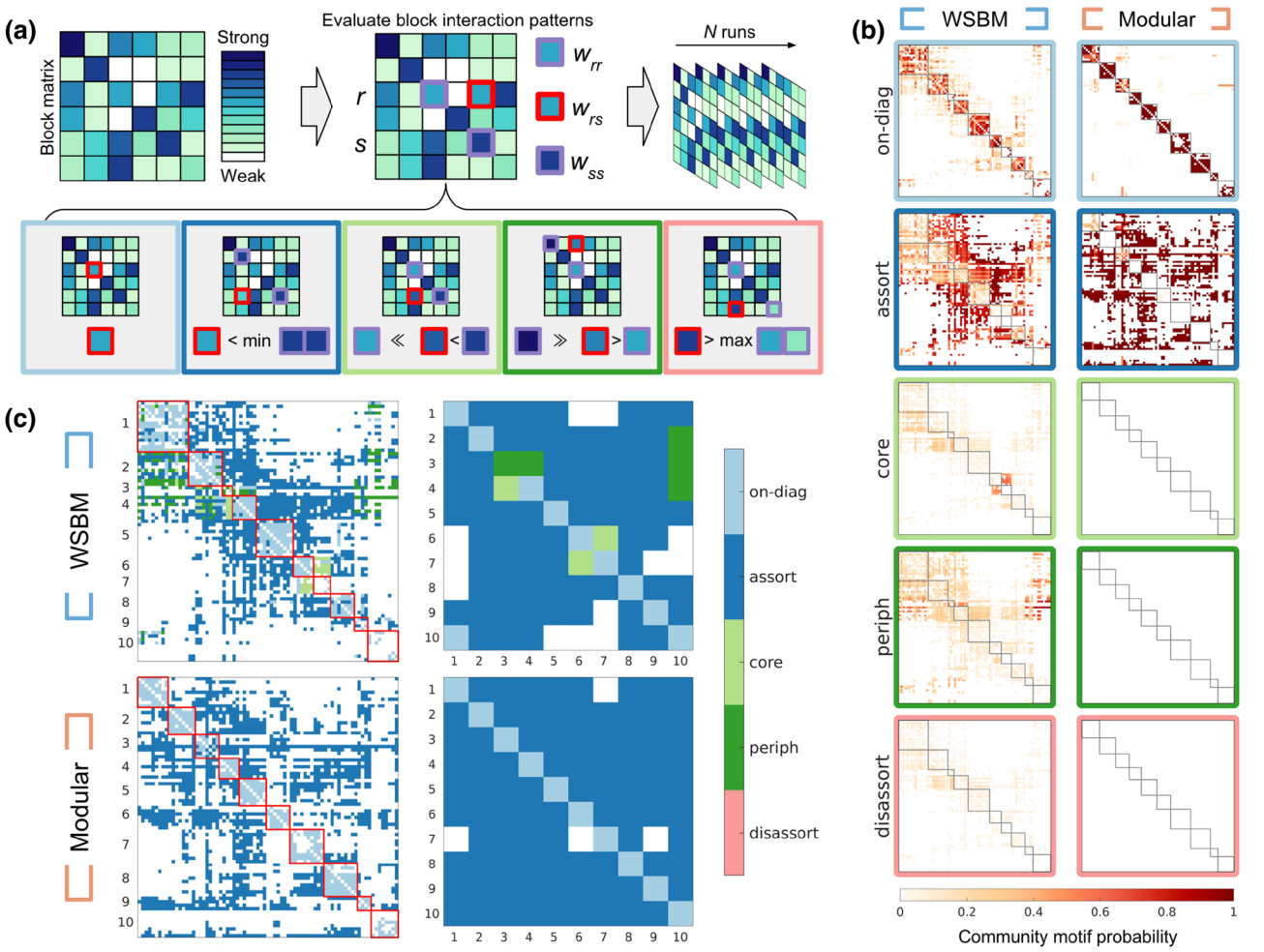

Fig. 5 Quantification of edge-wise community motif participation; **a** Diagram of steps used to evaluate community motif patterns; first, a matrix describing the average edge strength between blocks is obtained; second, the between-block relationships are labeled as either on-diagonal (light blue), assortative (dark blue), core (light green), periphery (dark green), or disassortative (salmon); third, these labels are assessed across multiple community structures; **b** A visualization of the edge-wise probability of participating in each community motif at $k=10$; across modular communities at this scale, there are no core, periphery, nor disassortative community motifs identified; **c** Left: each edge is colored according to the community motif it is most likely to participate in; Right: blocks are colored by the mode community motif for each block interaction; *on-diag* on-diagonal, *assort* assortative, *periph* periphery, *disassort* disassortative

Table 3 Top 10 most probable edges for core, periphery, and disassortative community motif participation across WSBM community structures; *i* indicates row (source), and *j* indicates column (target) for entry in the rat cortex connectome adjacency matrix

	Core			Periphery			Disassortative		
	i	*j*	Probability	*i*	*j*	Probability	*i*	*j*	Probability
1	VISp	VISlla	0.5827	ENTl	MOB	0.9307	ORBm	PL	0.2893
2	VISam	VISlla	0.5827	ENTl	AOB	0.9293	ORBv	ORBvl	0.284
3	VISp	VISll	0.5827	ENTm	IG	0.9133	MOs	ORBvl	0.2707
4	VISam	VISll	0.5827	ENTl	IG	0.9013	ECT	ORBvl	0.2707
5	VISp	VISli	0.5813	ENTl	FC	0.8973	CLA	ORBvl	0.2453
6	VISam	VISli	0.5813	ENTm	DG	0.868	ORBv	ORBl	0.2427
7	VISpm	VISli	0.5813	ENTl	DG	0.856	ORBm	ORBl	0.2427
8	VISal	VISlm	0.5813	ENTl	CA3	0.8427	MOs	ORBl	0.2387
9	VISp	VISlm	0.5813	ENTm	CA2	0.824	ECT	ORBl	0.2213
10	VISam	VISlm	0.5733	ENTl	CA2	0.8013	CLA	ORBl	0.216

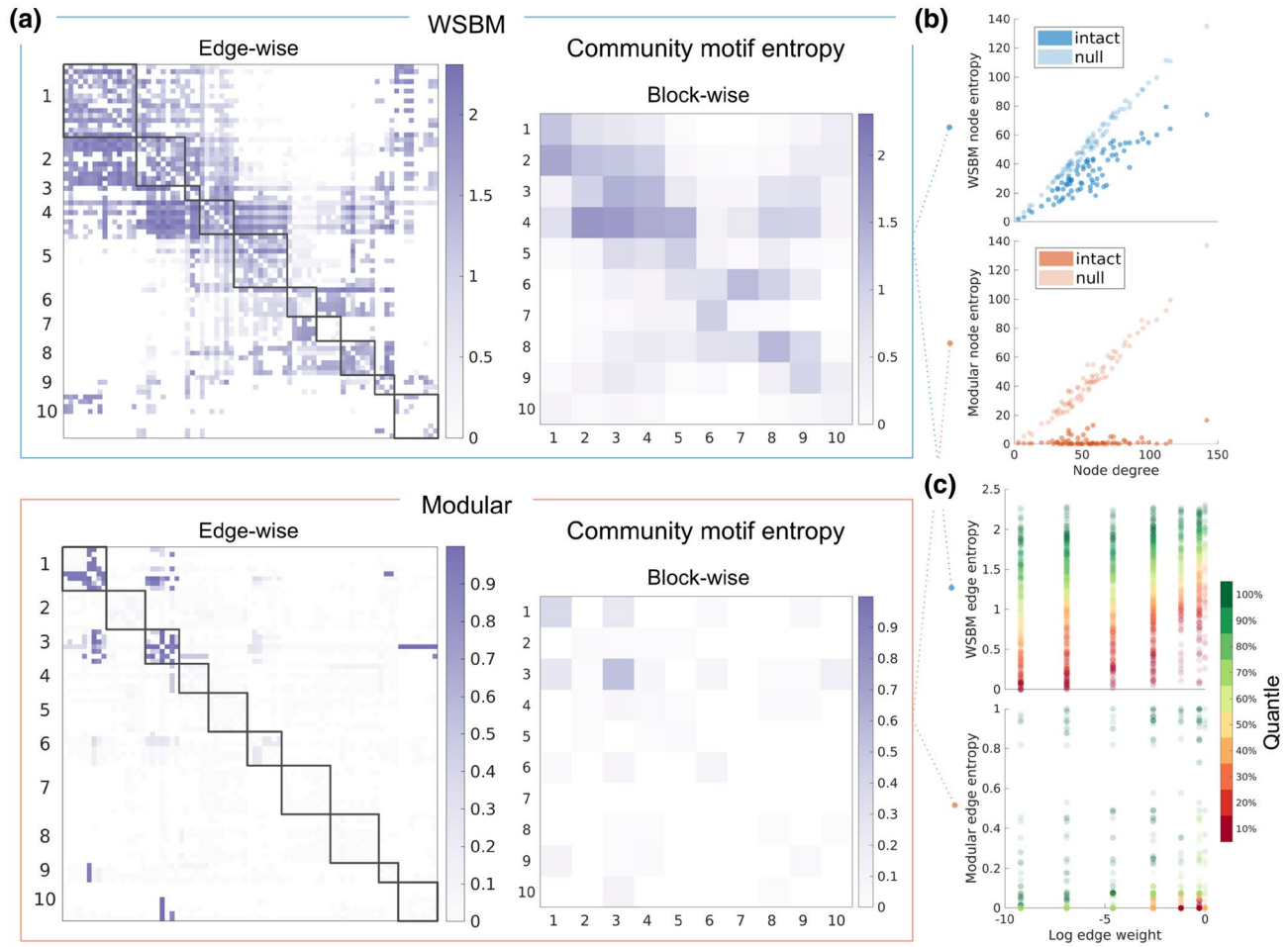

Fig. 6 Visualization of community motif entropy measure, and its relationship to node strength and edge weight; **a** Adjacency and block matrices of community motif entropy; **b** Scatterplot of node strength versus node entropy for both the WSBM and modular models; **c** Scatterplot of log edge weight versus edge entropy measurement, colored by the edge weight quantile; *quantile computed within each unique edge weight

correlate with log edge weight (Fig. 6c); the WSBM correlation is reliably greater than the modular correlation across bootstrapped samples (bootstrapped difference of means, 10^4 iterations, $p < 10^{-4}$). All correlations reported are non-parametric Spearman's rank correlations.

Here, we analyzed the one-hemisphere rat cerebral cortex brain. We also performed these analyses on a version of the data containing commissural connections and a second hemisphere. These analyses rendered analogous findings when comparing the WSBM and modular approaches (see Supplemental Information: *Analysis for two-hemisphere data*).

Discussion

This article describes a framework for fitting a blockmodel to the rat cortex connectome, represented as a weighted and directed connection matrix. First, we demonstrate how the blockmodel framework can be used to construct a consensus community structure from many plausible partitions. We compare the resulting consensus partition to another approach, more commonly used in the field, based on modularity maximization. We then compare the generative capabilities of these two different consensus community approaches. To gain a deeper understanding of the ensemble of partitions created by WSBM and modularity maximization, we analyze the variation in community structure configurations across many runs of community detection. Overall, leveraging these analyses, we observe features specific to the way that the WSBM and modular algorithms parse the rat cortex connectome.

The consensus community structure derived by WSBM parses the rat cerebral cortex in a manner that, in some respects, significantly differs from the partition resulting from modularity maximization. The WSBM community structure captures non-modular aspects, such as block

interactions classified as core and periphery (Fig. 4c) in addition to strong off-diagonal block interactions (e.g., intermodular interactions 4 → 2, 6 → 7, and 7 → 6). The 4 → 2 interaction links two communities that are highly enriched in putative hub and rich club areas, identified in previous work (Swanson et al. 2017). The 6 → 7 and 7 → 6 interactions link two communities dominated by visual sensory areas, one containing areas that are mutually densely connected (community 6; VISrl, VISal, VISp, VISam, VISpm), the other containing areas that are mutually sparsely connected (community 7; VISlla, VISll, VISli, VISlm, VISpl).

Other aspects of the WSBM community structure are significantly modular, and node groupings resemble those detected by modularity maximization. In a previous report using effectively the same data, a symmetric arrangement of three modules per hemisphere was identified using modularity maximization (Swanson et al. 2017): a lateral module consisting of perceptive systems related to interactions with the environment such as visual, auditory, and somatosensory areas; a ventromedial module containing regions involved in visceral monitoring and memory; and a dorsomedial module containing regions that are mainly associated with executive function. In this paper, we used modularity maximization to identify a consensus partition with $k = 10$ modules (intended to serve as a point of comparison to the 'optimal' WSBM solution). Despite the much larger set of modules, the modular communities 1, 3, 6, 9, and 10 mostly recapitulate the *Swanson2017* module 1, 5 and 7 the *Swanson2017* module 2, and 4 and 8 the *Swanson2017* module 3. Indeed, as observed when applying multiresolution consensus clustering on rat sub-connectomes (Swanson et al. 2018), finer-scale modular partitions generally represent hierarchical subdivisions of modules identified at coarser scales. Notably, even though the WSBM covers a much wider range of possible topologies that are accessed by modularity maximization, the overall WSBM partitioning scheme is less distant from modular community structure than chance, and it exhibits modularity, as indexed by the Q-metric, at levels far above those seen in random networks.

We demonstrate that a generative model based on the WSBM community structure produces synthetic networks with several network statistic properties that match the original network more closely than those obtained from modular synthetic networks. This implies that community structure formed by the WSBM can generate higher fidelity synthetic data. This capability could be explored further in future studies for creating surrogate brain networks that consider community structure information. The WSBM better matches the binary degree and weighted degree (strength) distributions, demonstrating its superior capability to model the existence of connections and their weights. On the other hand, both methods perform worst at generating synthetic networks with accurate clustering coefficient distributions; a result that comports with previous blockmodeling studies (Pavlovic et al. 2014; Faskowitz et al. 2018). Both community structures are non-trivially organized with regard to their generative capacities, as randomly permuting the block-interaction significantly decreases their generative performance (Fig. 3b).

When we fit the WSBM many times, we observe many ways in which the rat cortex connectome is parsed into plausible communities. To quantify this variation, we measure the proportion of times edges participate in specific community motifs (Betzel et al. 2018), across 750 runs of community detection. Across many runs of WSBM community detection, we find evidence of all five community motif configurations. More than 99% of the nonzero edges participate in at least two types of community motifs. In contrast, across many runs of modularity maximization, we observe only on-diagonal and assortative motifs. This analysis highlights complementary strengths of each community structure model: WSBM flexibly identifies communities based on various statistical patterns whereas modularity maximization reliably identifies communities with strong-within and weak-between topologies.

The probabilities of participating in community motifs demonstrate how connections of some brain areas might influence the structure of the communities that are formed. We observe how certain edges are repeatedly placed by the WSBM within the on-diagonal blocks, such as the edges within communities 5 and 6, communities composed of predominantly somatosensory, auditory, and visual areas. Numerous edges linking the visual community 6 to visual community 7 are classified as participating in core motifs. Edges between medial/lateral entorhinal areas and areas of the olfactory bulb and hippocampus are most likely classified as participating in peripheral motifs; previously, the medial and lateral entorhinal areas were considered candidate hub and rich club nodes (Swanson et al. 2017). While we do not find strong evidence of disassortative topologies across a majority of the WSBM, we note that the edges most likely to be disassortative all involve subdivisions of the orbital region of the rat cortex, as well as putative hub and rich club areas.

Across many recovered community structures, the WSBM partitions vary more than the modular partitions (Fig. 2c). We quantify this variation with the community motif entropy and observe how this entropy is organized across the nodes and edges of the rat cortex connectome (Fig. 6). Entropy is highly related to node degree when partitions are random. When the brain network is partitioned into a plausible community structure, we observe that entropy is systematically reduced relative to the random configuration. However, this reduction in entropy does not necessarily correlate with degree (Supplemental Fig. 2); the entropy decreases the most for nodes of the visual areas for both

methods. Across modular partitions, edge-wise entropy is mostly contained in connections between communities 1 and 3, which signal that node assignments between these communities are likely to exchange with one another; indeed, these two WSBM communities are placed within the same *Swanson2017* module, indicating their mutual affinity. This concurs with the modular agreement matrix, which also indicated this possibility (Supplemental Fig. 1). A future direction of investigation would be to evaluate how such structural characteristics could relate to patterns of brain function. In a similar analysis, it was shown that the diversity community motif patterns correlated with individual difference in human task performance (Betzel et al. 2018). We note that variability of the identified partitions is in part based on input of the network data and the stochasticity of the algorithm. Therefore, these results should be interpreted as variability relative to the community detection methods employed. We repeated these analyses with an alternative modularity maximization algorithm to demonstrate this (Supplemental Fig. 9).

The analyses reported in this paper add to a growing body of work indicating that a single community partition of brain data provides only an incomplete understanding of the brain's mesoscale organization. Instead, a more complete account of communities should consider multiple scales (Jeub et al. 2018; Yeh et al. 2018; Akiki and Abdallah 2019), the possible 'fuzziness' of partitions (Moyer et al. 2015a, b; Najafi et al. 2016), or build consensus structures from the data (Lancichinetti and Fortunato 2012, Faskowitz et al. 2018; Kurmukov et al. 2018). Ensemble approaches to network communities take into account that (1) community structure can vary across multiple runs of the same community detection algorithm (Shinn et al. 2017; Betzel et al. 2019); (2) different annotations can afford different perspectives on the same data (Peel et al. 2017); and (3) different community detection algorithms maximize different criteria (Schaub et al. 2017). This idea carries over to the WSBM framework. Any single WSBM community structure is likely to be just one of many plausible partitions of the data, in a similar manner to the degeneracy of the modularity landscape (Fortunato and Barthelemy 2007; Good et al. 2010). Here, we outline analytical approaches demonstrating that a brain network's community structure may be more than a grouping of nodes based on mutual density of connections. The identification of the community structure of a brain network reflects specific algorithmic goals and represents one of many plausible divisions of the network. By analyzing information across ensembles of network partitions, across scales and under varying definitions of what constitutes a 'community', we can achieve a fuller picture of the architecture of brain networks.

The understanding of mesoscale organization of the rat cerebral cortex will continue to develop as the connectivity data become more complete and the community detection algorithms grow more sophisticated. New connections continue to be added to the rat connectome dataset, including association fibers (Swanson et al. 2017), connections to the endbrain (Swanson et al. 2018), and thalamic nuclei connections (Swanson et al. 2019). We provide further analyses of the two-hemisphere rat cerebral cortex connectome in Supplemental Information and report analogous results to the one-hemisphere findings. Notably, the two-hemisphere WSBM consensus community structure is symmetric across the hemispheres, reflecting a limitation of the underlying data. Future work on the organization of the rat connectome could focus on inferring mesoscale structure with added metadata (Hric et al. 2016) such as neurochemical relationships (Noori et al. 2017) or using alternative node definitions or informatically collated data (Schmitt and Eipert 2012). Such added information could enhance our understanding of the potential functions identified communities might play. Further, algorithmic advances in community detection could aid in inferring the rat brain mesoscale organization. The WSBM algorithm recovered substantially less unique partitions at high values of k (i.e., $k \geq 17$; Supplemental Fig. 4), but future SBM algorithms could be more efficient for larger networks (Peixoto 2018). Alternatively, future work on the variability of plausible partitions could be conducted using different community detection criteria (Chen et al. 2013; Schaub et al. 2017).

Acknowledgements O.S. acknowledges funding support by the National Institutes of Health (R01 AT009036-01 and R01 MH122957-01). This material is based on the work supported by the National Science Foundation Graduate Research Fellowship under Grant No. 1342962 (J.F.). Any opinions, findings, and conclusions or recommendations expressed in this material are those of the author(s) and do not necessarily reflect the views of the National Science Foundation. Supercomputing was supported in part by Lilly Endowment, Inc., through its support for the Indiana University Pervasive Technology Institute, and in part by the Indiana METACyt Initiative. The Indiana METACyt Initiative at IU was also supported in part by Lilly Endowment, Inc. We would like to thank Christopher Aicher and Aaron Clauset for implementing and hosting the WSBM code package.

Compliance with ethical standards

Conflict of interest The authors declare no conflicts of interest.

References

Aicher C, Jacobs AZ, Clauset A (2013) Adapting the stochastic block model to edge-weighted networks. arXiv:1305.5782

Aicher C, Jacobs AZ, Clauset A (2014) Learning latent block structure in weighted networks. J Complex Netw 3(2):221–248

Airoldi EM, Blei DM, Fienberg SE, Xing EP (2008) Mixed membership stochastic blockmodels. J Mach Learn Res 9:1981–2014

Akiki TJ, Abdallah CG (2019) Determining the hierarchical architecture of the human brain using subject-level clustering of functional networks. https://doi.org/10.1101/350462

Alexander-Bloch A, Lambiotte R, Roberts B, Giedd J, Gogtay N, Bullmore E (2012) The discovery of population differences in network community structure: new methods and applications to brain functional networks in schizophrenia. NeuroImage 59(4):3889–3900

Bassett DS, Sporns O (2017) Network neuroscience. Nat Neurosci 20(3):353–364

Bassett DS, Greenfield DL, Meyer-Lindenberg A, Weinberger DR, Moore SW, Bullmore ET (2010) Efficient physical embedding of topologically complex information processing networks in brains and computer circuits. PLoS Comput Biol 6(4):e1000748

Battiston F, Guillon J, Chavez M, Latora V, De Vico Fallani F (2018) Multiplex core–periphery organization of the human connectome. J R Soc Interface 15(146):20180514

Baum GL, Ciric R, Roalf DR, Betzel RF, Moore TM, Shinohara RT et al (2017) Modular segregation of structural brain networks supports the development of executive function in youth. Curr Biol 27(11):1561–1572

Betzel RF, Bassett DS (2017) Multi-scale brain networks. Neuroimage 160:73–83

Betzel RF, Avena-Koenigsberger A, Goni J, He Y, de Reus MA, Griffa A, Sporns O (2016) Generative models of the human connectome. Neuroimage 124(Pt A):1054–1064

Betzel RF, Medaglia JD, Papadopoulos L, Baum GL, Gur R, Gur R, Bassett DS (2017) The modular organization of human anatomical brain networks: accounting for the cost of wiring. Netw Neurosci 1(1):42–68

Betzel RF, Medaglia JD, Bassett DS (2018) Diversity of meso-scale architecture in human and non-human connectomes. Nat Commun 9(1):346

Betzel RF, Bertolero MA, Gordon EM, Gratton C, Dosenbach NUF, Bassett DS (2019) The community structure of functional brain networks exhibits scale-specific patterns of inter- and intra-subject variability. NeuroImage 202:115990

Blondel VD, Guillaume J-L, Lambiotte R, Lefebvre E (2008) Fast unfolding of communities in large networks. J Stat Mech Theory Exp 10:P10008

Bota M, Swanson LW (2007) Online workbenches for neural network connections. J Comp Neurol 500(5):807–814

Bota M, Sporns O, Swanson LW (2015) Architecture of the cerebral cortical association connectome underlying cognition. Proc Natl Acad Sci 112(16):E2093–E2101

Bullmore E, Sporns O (2012) The economy of brain network organization. Nat Rev Neurosci 13(5):336–349

Chen M, Nguyen T, Szymanski BK (2013) On measuring the quality of a network community structure. In: 2013 international conference on social computing. IEEE, pp 122–127

Contreras JA, Avena-Koenigsberger A, Risacher SL, West JD, Tallman E, McDonald BC et al (2019) Resting state network modularity along the prodromal late onset Alzheimer's disease continuum. NeuroImage 22:101687

Crossley NA, Mechelli A, Vértes PE, Winton-Brown TT, Patel AX, Ginestet CE, Bullmore ET (2013) Cognitive relevance of the community structure of the human brain functional coactivation network. Proc Natl Acad Sci 110(28):11583–11588

Faskowitz J, Yan X, Zuo X-N, Sporns O (2018) Weighted stochastic block models of the human connectome across the life span. Sci Rep 8(1):12997

Fortunato S, Barthelemy M (2007) Resolution limit in community detection. Proc Natl Acad Sci 104(1):36–41

Fortunato S, Hric D (2016) Community detection in networks: a user guide. Phys Rep-Rev Sect Phys Lett 659:1–44

Good BH, de Montjoye Y-A, Clauset A (2010) Performance of modularity maximization in practical contexts. Phys Rev E 81(4):046106

Harriger L, van den Heuvel MP, Sporns O (2012) Rich club organization of macaque cerebral cortex and its role in network communication. PLoS One 7(9):e46497

He Y, Lim S, Fortunato S, Sporns O, Zhang L, Qiu J, Zuo XN (2018) Reconfiguration of cortical networks in MDD uncovered by multiscale community detection with fMRI. Cereb Cortex 28(4):1383–1395

Holland PW, Laskey KB, Leinhardt S (1983) Stochastic blockmodels: first steps. Soc Netw 5(2):109–137

Hric D, Peixoto TP, Fortunato S (2016) Network structure, metadata, and the prediction of missing nodes and annotations. Phys Rev X 6(3):031038

Jeub LG, Sporns O, Fortunato S (2018) Multiresolution consensus clustering in networks. Sci Rep 8(1):3259

Karrer B, Newman ME (2011) Stochastic blockmodels and community structure in networks. Phys Rev E 83(1 Pt 2):016107

Kurmukov A, Ananyeva M, Dodonova Y, Gutman B, Faskowitz J, Jahanshad N, Zhukov L (2017) Classifying phenotypes based on the community structure of human brain networks. In: Graphs in biomedical image analysis, computational anatomy and imaging genetics. Springer, Cham, pp 3–11

Kurmukov A, Musabaeva A, Denisova Y, Moyer D, Gutman B (2018) Connectivity-driven brain parcellation via consensus clustering. In: Connectomics in neuroimaging. Springer, Cham, pp 117–126

Kwak H, Choi Y, Eom Y-H, Jeong H, Moon S (2009) Mining communities in networks: a solution for consistency and its evaluation. In: Proceedings of the 9th ACM SIGCOMM conference on Internet measurement conference. ACM, pp 301–314

Lancichinetti A, Fortunato S (2012) Consensus clustering in complex networks. Sci Rep 2:336

Meilă M (2007) Comparing clusterings—an information based distance. J Multivar Anal 98(5):873–895

Meunier D, Achard S, Morcom A, Bullmore E (2009) Age-related changes in modular organization of human brain functional networks. Neuroimage 44(3):715–723

Moyer D, Gutman B, Prasad G, Faskowitz J, Ver Steeg G, Thompson P (2015a) Blockmodels for connectome analysis. 11th International Symposium on Medical Information Processing and Analysis (SIPAIM 2015): 96810A-96810A-96819

Moyer D, Gutman B, Prasad G, Ver Steeg G, Thompson P (2015b) Mixed membership stochastic blockmodels for the human connectome. In: MICCAI–workshop on bayesian and graphical models for biomedical imaging

Munkres J (1957) Algorithms for the assignment and transportation problems. J Soc Ind Appl Math 5(1):32–38

Najafi M, McMenamin BW, Simon JZ, Pessoa L (2016) Overlapping communities reveal rich structure in large-scale brain networks during rest and task conditions. NeuroImage 135:92–106

Newman ME (2006) Modularity and community structure in networks. Proc Natl Acad Sci 103(23):8577–8582

Noori HR, Schöttler J, Ercsey-Ravasz M, Cosa-Linan A, Varga M, Toroczkai Z, Spanagel R (2017) A multiscale cerebral neurochemical connectome of the rat brain. PLoS Biol 15(7):e2002612

Park H-J, Friston K (2013) Structural and functional brain networks: from connections to cognition. Science 342(6158):1238411

Pavlovic DM, Vertes PE, Bullmore ET, Schafer WR, Nichols TE (2014) Stochastic blockmodeling of the modules and core of the Caenorhabditis elegans connectome. PLoS One 9(7):e97584

Peel L, Larremore DB, Clauset A (2017) The ground truth about metadata and community detection in networks. Sci Adv 3(5):e1602548

Peixoto TP (2018) Nonparametric weighted stochastic block models. Phys Rev E 97(1–1):012306

Rubinov M, Sporns O (2010) Complex network measures of brain connectivity: uses and interpretations. Neuroimage 52(3):1059–1069
Rubinov M, Ypma RJ, Watson C, Bullmore ET (2015) Wiring cost and topological participation of the mouse brain connectome. Proc Natl Acad Sci 112(32):10032–10037
Schaub MT, Delvenne J-C, Rosvall M, Lambiotte R (2017) The many facets of community detection in complex networks. Appl Netw Sci 2(1):4
Schmitt O, Eipert P (2012) neuroVIISAS: approaching multiscale simulation of the rat connectome. Neuroinformatics 10(3):243–267
Shih C-T, Sporns O, Yuan S-L, Su T-S, Lin Y-J, Chuang C-C, Chiang A-S (2015) Connectomics-based analysis of information flow in the drosophila brain. Curr Biol 25(10):1249–1258
Shinn M, Romero-Garcia R, Seidlitz J, Váša F, Vértes PE, Bullmore E (2017) Versatility of nodal affiliation to communities. Sci Rep 7(1):4273
Sohn Y, Choi MK, Ahn YY, Lee J, Jeong J (2011) Topological cluster analysis reveals the systemic organization of the Caenorhabditis elegans connectome. PLoS Comput Biol 7(5):e1001139
Sporns O (2011) The human connectome: a complex network. Ann NY Acad Sci 1224(1):109–125
Sporns O (2013) Making sense of brain network data. Nat Methods 10(6):491–493
Sporns O, Betzel RF (2016) Modular Brain Networks. Annu Rev Psychol 67:613–640
Sporns O, Tononi G, Kötter R (2005) The human connectome: a structural description of the human brain. PLoS Comput Biol 1(4):e42
Swanson LW, Sporns O, Hahn JD (2016) Network architecture of the cerebral nuclei (basal ganglia) association and commissural connectome. Proc Natl Acad Sci 113(40):E5972–E5981
Swanson LW, Hahn JD, Sporns O (2017) Organizing principles for the cerebral cortex network of commissural and association connections. Proc Natl Acad Sci 114(45):E9692–E9701
Swanson LW, Hahn JD, Jeub LGS, Fortunato S, Sporns O (2018) Subsystem organization of axonal connections within and between the right and left cerebral cortex and cerebral nuclei (endbrain). Proc Natl Acad Sci 115(29):E6910–E6919
Swanson LW, Sporns O, Hahn JD (2019) The network organization of rat intrathalamic macroconnections and a comparison with other forebrain divisions. Proc Natl Acad Sci 116(27):13661–13669
Tunç B, Verma R (2015) Unifying inference of meso-scale structures in networks. PLoS One 10(11):e0143133
van den Heuvel MP, Scholtens LH, de Reus MA (2016) Topological organization of connectivity strength in the rat connectome. Brain Struct Funct 221(3):1719–1736
Xiaoran Y, Cosma S, Jacob EJ, Florent K, Cristopher M, Lenka Z, Yaojia Z (2014) Model selection for degree-corrected block models. J Stat Mech 2014(5):P05007
Yeh F-C, Panesar S, Fernandes D, Meola A, Yoshino M, Fernandez-Miranda JC, Verstynen T (2018) Population-averaged atlas of the macroscale human structural connectome and its network topology. NeuroImage 178:57–68
Zhao T, Cao M, Niu H, Zuo X-N, Evans A, He Y, Shu N (2015) Age-related changes in the topological organization of the white matter structural connectome across the human lifespan. Hum Brain Mapp 36(10):3777–3792
Zingg B, Hintiryan H, Gou L, Song MY, Bay M, Bienkowski MS, Toga AW (2014) Neural networks of the mouse neocortex. Cell 156(5):1096–1111